Journal of Materials Chemistry C

PAPER

View Article Online
View Journal | View Issue

Cite this: J. Mater. Chem. C, 2017, 5, 4275

A low loading of grafted thermoplastic polystyrene strengthens and toughens transparent epoxy composites†

Hongbo Gu, *[a] Chao Ma,[a] Chaobo Liang,[b] Xudong Meng,[b] Junwei Gu*[b] and Zhanhu Guo [c]

Transparent epoxy composites strengthened and toughened by thermoplastic polystyrene grafted with epichlorohydrin (*g*-PS) have been prepared at low loading levels. The polymer backbone of PS was manipulated by the epoxide and hydroxyl groups confirmed by Fourier transform infrared spectroscopy (FT-IR), thermogravimetric analysis (TGA), and X-ray photoelectron spectroscopy (XPS). Contact angle and differential scanning calorimetry (DSC) tests indicated that the grafting process could decrease the surface tension and increase the compatibility between PS and epoxy resins. The effects of *g*-PS loading and the grafting process on both the viscosity of liquid epoxy resin suspensions as well as the physicochemical properties of cured epoxy composites have been systematically investigated. The cured *g*-PS/epoxy composites demonstrated an enhanced tensile strength (maximum of 97.4 MPa) compared to either cured pure epoxy (77.6 MPa) or PS/epoxy composites (79.1 MPa). The modulus of toughness for *g*-PS/epoxy composites reaches values of up to 355.9 MJ m^{-3}, which is respectively 176.6 and 141.1% higher than those for cured pure epoxy and PS/epoxy composites. The uniform *g*-PS distribution in the cured *g*-PS/epoxy composites was observed by scanning electron microscope (SEM). The glass transition temperature (T_g) of cured *g*-PS/epoxy composites was shifted to a higher temperature (increased by 16.3 °C) in the dynamic mechanical analysis (DMA) compared with that of cured pure epoxy (111.7 °C). The strong interfacial interaction obtained between *g*-PS and the epoxy matrix was responsible for the enhanced mechanical and thermal mechanical properties. This work provides a new insight into the investigation of interaction and compatibility between thermoplastic and thermoset materials.

Received 26th January 2017,
Accepted 28th March 2017

DOI: 10.1039/c7tc00437k

rsc.li/materials-c

1. Introduction

Epoxy resin, as one of the most classic and important thermosetting resins, is universally applied in adhesives,[1] electronic devices,[2] encapsulation,[3] laminates,[4] marine systems,[5] aerospace,[6] and coatings[7] due to its high tensile strength and Young's modulus, good thermal stability and thermal insulation, and excellent solvent resistance.[8] The incorporation of inorganic fillers, such as fibers, particles with micrometric or nanometric dimensions, into epoxy has been a common way to fabricate high-performance materials in modern industries.[9] Normally, epoxy is an insoluble and infusible thermoset with low fracture extensibility and high brittleness. Therefore, it is important to strengthen and toughen the cured epoxy for more extensive applications. Recently, reactive elastomers, rubbers, and high performance thermoplastic polymers have been used to resolve these problems with epoxy.[10,11] For example, Francis *et al.*[12] tried thermoplastic poly(ether ether ketone) (PEEK) as an effective toughener for cured epoxy. Shukla *et al.*[13] prepared carboxyl-terminated polybutadiene (CTPB) liquid rubber to blend with epoxy and obtained a toughness-increased material with a CTPB loading of up to 15 wt%. Upon further increasing CTPB loadings, the toughness started to decline. Sinh *et al.*[14] used an amino end-capped aromatic liquid crystalline copoly(ester amide) (LCP) to mix with epoxy and obtained a 30% improvement in tensile strength and around 10% increase in toughness compared with pure epoxy. Roy *et al.*[15] developed a simple procedure for the preparation of core–shell poly(dimethylsiloxane)–epoxy microspheres (CPR) *via* a suspension polymerization route and

[a] Shanghai Key Lab of Chemical Assessment and Sustainability, School of Chemical Science and Engineering, Tongji University, Shanghai 200092, P. R. China. E-mail: hongbogu2014@tongji.edu.cn
[b] MOE Key Laboratory of Space Applied Physics and Chemistry, Shaanxi Key Laboratory of Macromolecular Science and Technology, Department of Applied Chemistry, School of Science, Northwestern Polytechnical University, Xi'an, Shaanxi, 710072, P. R. China. E-mail: gjw@nwpu.edu.cn
[c] Integrated Composites Laboratory (ICL), Department of Chemical & Biomolecular Engineering, University of Tennessee, Knoxville, Tennessee, 37966, USA

† Electronic supplementary information (ESI) available. See DOI: 10.1039/c7tc00437k

demonstrated its potential as an effective toughening agent for thermosetting epoxy. The impact strength and fracture energy were respectively increased by 148 and 70% by addition of 5 wt% loading of CPR. However, the effectively increased toughness has been achieved only at a high loading of CPR. Consequently, the high cost and difficulty in handling of CPR severely limit their applications in preparing high-performance epoxy composites.

Polystyrene (PS), one of the most commonly used thermoplastic polymers, has been widely deployed in applications including protective packaging (such as CD and DVD cases),[16] containers (such as ''clamshells''),[17] lids, bottles, trays, tumblers,[18] and disposable cutlery. Nevertheless, it biodegrades very slowly, which makes PS an increasingly abundant pollutant littered in the environment, particularly along the shores and waterways in the Pacific Ocean.[19] Therefore, how to use it effectively as well as recycle and reuse it is a focus of controversy among environmentalists. Some research studies have been carried out with the focus on mixing PS with epoxy. On the one hand, PS has good processability and low production cost, which provides epoxy with new mechanical performance. On the other hand, it also offers a new method for recycling and reusing PS wastes. From the phase separation and conversion point of view, Hoppe *et al.*[20] suggested that PS with an epoxy monomer and tertiary amine (PS/epoxy/BDMA) could be used to yield transparent epoxy coatings toughened by PS particles. More recently, Sun *et al.*[21] fabricated aminated PS spheres to prepare epoxy composites and obtained an increased tensile strength (increased by 25.6%) and toughness (increased by 84.3%). However, they used a very high loading of PS of up to 15 wt%, which may cause a decrease in handling. Therefore, the question of how to avoid phase separation to obtain a homogenous dispersion with low loading of PS strengthened and toughened epoxy composites still needs to be addressed.

In order to resolve these drawbacks and provide a new method for the potential application of reusing and recycling PS, in the present work, the epoxy composites reinforced with a low loading of epichlorohydrin grafted PS have been successfully prepared. It turned out that the low loading of PS could make epoxy composites transparent. The interaction between grafted PS and the epoxy matrix was elaborated on the basis of contact angle and differential scanning calorimetry (DSC) tests. The effect of grafted PS loadings, grafting process and temperature change on the viscosity of liquid epoxy resin was investigated in detail. A study on the mechanical and thermal mechanical property tests of cured epoxy composites has been conducted. The fracture surface of cured epoxy composites was observed using scanning electron microscope (SEM). In addition, the composites filled with pure PS powders were also prepared for comparison. In consequence, this work made it possible to avoid phase separation during the preparation process of PS/epoxy composites and obtain a uniform dispersion of PS within an epoxy matrix, which further led to the enhanced tensile strength and modulus of toughness.

2. Experimental

2.1 Materials

Epon 862 (bisphenol F epoxy) and the curing agent EK3402 were purchased from Hexion Inc. The molecular structures of these chemicals are shown in Scheme S1 (ESI†). Polystyrene (PS, $M_w \approx 57\,700$) was supplied by Taizhou Suosi Education Equipment Co., Ltd. Ethyl acetate ($C_4H_8O_2$, $\geq$99.5%), acetone (CH_3COCH_3, $\geq$99.5%), cyclohexane (C_6H_{12}, $\geq$99.5%), anhydrate aluminum trichloride ($AlCl_3$, $\geq$99.0%), epichlorohydrin (C_3H_5ClO, $\geq$99.0%), dimethylformamide (DMF, C_3H_7NO, $\geq$99.5%), anhydrous ethanol and ethanol ($C_6H_{12}O$, 95%, v/v) were provided by Sinopharm Chemical Reagent Co., Ltd. The as-received PS granules (1 g) were dissolved in 25 mL of DMF solution under magnetic stirring and heated to 100 °C. After cooling down to room temperature, the obtained pure PS powders were freeze-dried for 12 hours. Then the dried pure PS powders were ground in a mortar and pestle and sieved to have a particle diameter of less than 75 μm for further usage. Other chemicals were used as-received without any further treatment.

2.2 Epichlorohydrin grafted PS (*g*-PS) fabrication

5 wt% of PS granules were dissolved in 25 mL of mixed solvent containing ethyl acetate (11 mL), acetone (5 mL) and cyclohexane (9 mL) at room temperature. Then 5 mL of anhydrous ethanol with 11 wt% of $AlCl_3$ was added into the above solution for 30 min of magnetic stirring. After that, 1.05 mL of epichlorohydrin (the volume of epichlorohydrin was calculated based on the polymerization degree of as-received PS, which ensured the maximum grafting ratio of epichlorohydrin in a bid for the best compatibility between *g*-PS and epoxy matrix) was dripped into the solution followed by another 30 min of magnetic stirring. The obtained *g*-PS powders were washed with ethanol under sonication five times to remove the extra unreacted epichlorohydrin, $AlCl_3$ and solvent. Then, the clean *g*-PS powders were filtered by using a Buchner funnel and freeze-dried for 12 hours. Finally, the dried powders were ground in a mortar and pestle and sieved to be of particle diameter less than 75 μm for preparing epoxy composites.

2.3 Preparation of PS/epoxy composites

2.3.1 PS/epoxy resin composite suspensions. Epoxy resin suspensions with 0.5, 1.0, 1.5, 2.0, and 2.5 wt% loadings of *g*-PS and 0.5 wt% loading of pure PS powders were prepared (as the loading of pure PS powders was increased, the viscosity of epoxy suspensions increased rapidly and many bubbles formed during the mechanical stirring. Therefore, the higher loadings of pure PS powders were not used in this work.). Both *g*-PS and pure PS powders were wetted by epoxy resin overnight without any disturbance. Then the suspension was mechanically stirred for one hour (600 rpm, D2004W, Shanghai Mei YIngpu instrument and Meter Manufacturing Co., Ltd) at 25 °C.

2.3.2 Curing of PS/epoxy composites. The curing agent EK3402 was added into epoxy resin or the above prepared PS/epoxy resin suspensions with a resin/curing agent weight ratio of 100/26.5 as recommended by Hexion Inc. and mechanically

stirred (200 rpm) for one hour. Then the solution was heated to 50 °C in a water bath and maintained for some time for the increase of viscosity to occur (For the *g*-PS/epoxy suspensions, at temperatures higher than 50 °C, the *g*-PS and epoxy resin started to exhibit severe phase separation. This may be due to the fact that the glass transition temperature (T_g) of PS was close to 70–80 °C and the viscosity of epoxy resin decreased with increasing temperature. Therefore, 50 °C was chosen as the mixing temperature of epoxy suspensions with the curing agent.). Finally, the well-mixed solutions were poured into silicon rubber molds, cured at 120 °C for 5 hours and cooled down to room temperature naturally. The cured pure epoxy was also synthesized following the same procedure without adding PS/*g*-PS powders for comparison.

2.4 Characterization

The chemical structures of pure PS and *g*-PS were measured using Fourier transform infrared spectroscopy (FT-IR, Thermo Scientific, Thermo Nicolet NEXUS with an ATR accessory) in the range of 500 to 4000 cm^{-1} with a resolution of 4 cm^{-1} and X-ray photoelectron spectroscopy (XPS, Kratos AXIS Ultra DLD spectrometer, Al Kα ($h\nu$ = 1486.6 eV) radiation as the excitation source under an anode voltage of 12 kV and an emission current of 10 mA). The high resolution C1s peaks of pure PS and *g*-PS were deconvoluted into the components composed of a Gaussian line shape Lorentzian function (Gaussian = 80%, Lorentzian = 20%) on a Shirley background. The TGA and DSC tests were performed at a heating rate of 5 °C min^{-1} under an air flow rate of 60 mL min^{-1} from 25 to 800 °C. The contact angle between pure PS or *g*-PS powders and epoxy resin monomers was measured using a CA100B from Shanghai Innuo Precision Instruments Co., Ltd at 25 °C. The pure PS or *g*-PS powders were pressed in a disc pellet in a hydraulic press (769YP-15A, Tianjin KEQI High & New Tech Corporation). Then 5 μL of the epoxy resin monomers were dripped on the pellet using a micropipette for the test. For accuracy, the measurements were repeated five times on different pieces of the same sample. The morphologies of *g*-PS and fracture surfaces of epoxy composites were observed on a field emission scanning electron microscope (FE-SEM, Hitachi S-4800 system). The SEM specimens were prepared by sputtering a thin gold layer, which was about 3 nm thick.

The rheological properties of liquid epoxy suspensions with pure PS or *g*-PS powders were determined in a rheometer (model: RS3CPS23OLS, Brookfield Engineering Laboratories, Inc.). The tests were carried out in a cone-plate geometry with a diameter of 25 mm and a truncation of 55 μm. In order to study the effect of temperature change on the viscosity, the steady state flow procedure was applied to perform the measurements at 25, 40 and 50 °C at a shear rate of 1 to 1000 s^{-1}, respectively. The specimens placed between the cone and the plate reached equilibrium for about 100 seconds before each test.

The tensile tests were carried out by using the dog-bone shaped samples following the American Society for Testing and Materials (ASTM, 2002, standard D412-98a) in a unidirectional tensile test machine (Shanghai Xieqiang Instrument Technology Co. Ltd). A crosshead speed of 1 mm min^{-1} was used and the strain (%) was calculated by dividing the jogging displacement with the initial gauge length (26 mm). Dynamic mechanical analysis (DMA) was conducted in the DMA multi-frequency–strain mode by using TA DMA Q800 with a frequency of 1 Hz and a heating rate of 5 °C min^{-1} in the temperature range of 25 to 330 °C. The sample dimensions were 60 × 10 × 4 mm^3.

3. Results and discussion

3.1 Characterization of *g*-PS

Fig. 1(A) shows the FTIR spectra of *g*-PS and pure PS from 500 to 4000 cm^{-1}. It is found that the FTIR spectrum of *g*-PS has an obvious difference from that of pure PS within the wavenumber range of 3200 to 3650 cm^{-1} as indicated by the blue color. This broad peak in the FTIR spectrum of *g*-PS is due to the stretching of O–H. Fig. 1(B) depicts the TGA decomposition profiles of pure PS and *g*-PS. The pure PS exhibits only one stage of weight loss from 300 to 400 °C due to the thermal degradation of the hexagonal carbon from the PS polymer.[22] For the *g*-PS, the weight loss between 200 and 300 °C in the curve is attributed to the grafted functional groups on the *g*-PS polymer backbone, which corresponds to the degradation of C–O–C groups.[23] The FTIR and TGA tests confirm that there are hydroxyl and epoxide groups on the polymer backbone of *g*-PS.

The surface functional groups were further investigated using XPS analysis. The high resolution C1s XPS spectra of pure PS and *g*-PS are shown in Fig. 1(C) and (D), respectively. The C1s peak of pure PS is deconvoluted into two major components with peaks at 284.7 and 285.4 eV, which are attributed to C=C of the benzene ring and C–C of the PS polymer backbone, respectively, as seen in Fig. 1(C). However, the C1s spectrum of *g*-PS is different from that of pure PS, in which the four components are fitted, Fig. 1(D). The highest peak located at 284.8 eV is assigned to the C=C of the benzene ring. The binding energies of 285.7, 286.3, and 287.2 eV are attributed to C–C, C–OH, and C–O–C, respectively.[24] This confirms that after the grafting process, the hydroxyl and epoxide groups are present on the *g*-PS polymer backbone, which is consistent with the results obtained from FTIR and TGA. The content of the hydroxyl and epoxide groups is 17.1 and 6.2%, respectively. The total grafting ratio of epichlorohydrin on the PS polymer is around 23.3%. The SEM image of *g*-PS is shown in Fig. S1(a) (ESI†).

3.2 Interaction exploration between *g*-PS and epoxy resin

3.2.1 Contact angle. Fig. 2 indicates the measured contact angles between pure PS/*g*-PS and epoxy resin droplet at room temperature. It is found that the contact angle between *g*-PS and epoxy resin (43.6°) is lower than that between pure PS and epoxy resin (50.9°), indicating increased compatibility between *g*-PS and epoxy resin after the grafting process. Normally, the surface tension for the solid–liquid (γ_{sl}) phase, and the liquid–air (γ_{lg}) phase can be calculated through the contact angle results by the following relationship as shown in eqn (1):[25]

$$\gamma_{sl} = \frac{\gamma_{lg}}{2}\left(\sqrt{1+\sin^2\theta} - \cos\theta\right) \quad 0 < \theta < 180^\circ \qquad (1)$$

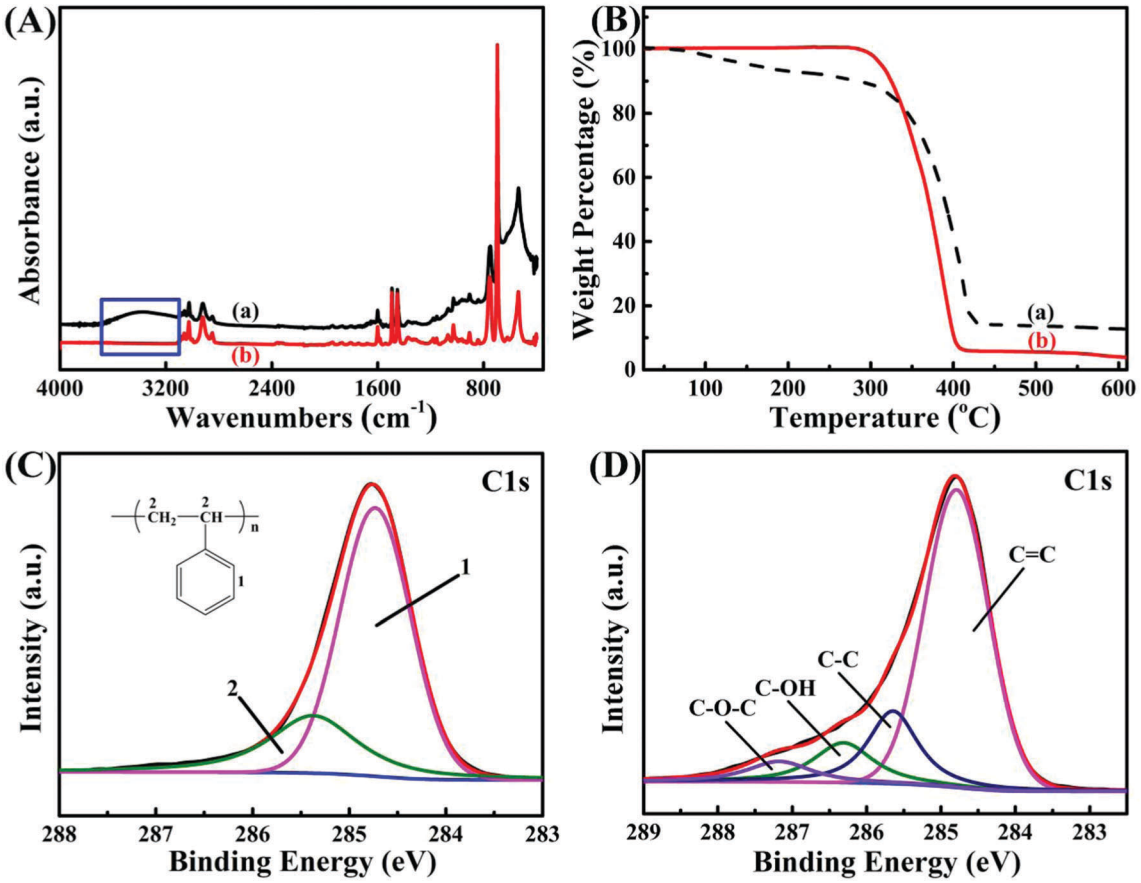

Fig. 1 (A) FT-IR spectra of (a) *g*-PS, (b) pure PS; (B) TGA curves of (a) *g*-PS, (b) pure PS; high resolution C1s XPS spectra of (C) pure PS; and (D) *g*-PS.

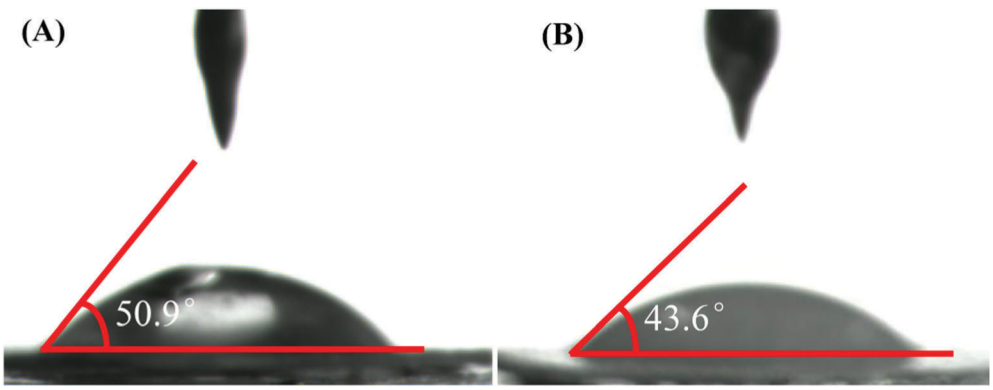

Fig. 2 Contact angle of epoxy resins with (A) pure PS, and (B) *g*-PS at room temperature.

where θ is the contact angle, and γ_{lg} = 72 N m^{-1}. The calculated γ_{sl} for the *g*-PS and the epoxy resin phase is 17.7 × 10^{-3} N m^{-1}, which is much lower than that for the PS and the epoxy resin phase (22.9 × 10^{-3} N m^{-1}). Generally, the lower the γ_{sl} value, the better the wettability between the liquid and the solid phase,[26] which means that after grafting functional groups on the polymer backbone of PS, the interaction between *g*-PS and epoxy resin is significantly improved.

3.2.2 DSC test. Fig. S2 (ESI†) shows the DSC curves of epoxy resin monomers, and epoxy resin suspensions with pure PS and *g*-PS. For the epoxy resin suspension with pure PS, Fig. S2(b) (ESI†), the baseline is very straight and similar to that of the pure epoxy resin monomer, Fig. S2(c) (ESI†), indicating that no chemical reaction occurred between pure PS and epoxy. However, the baseline is not that straight and a broad exothermic peak appears in the epoxy resin suspension with *g*-PS, Fig. S2(a) (ESI†), indicating a chemical reaction between the functional groups on the *g*-PS polymer backbone and the epoxy resin monomers. This means that the functional groups on *g*-PS could boost the interaction between *g*-PS and epoxy resin.[27]

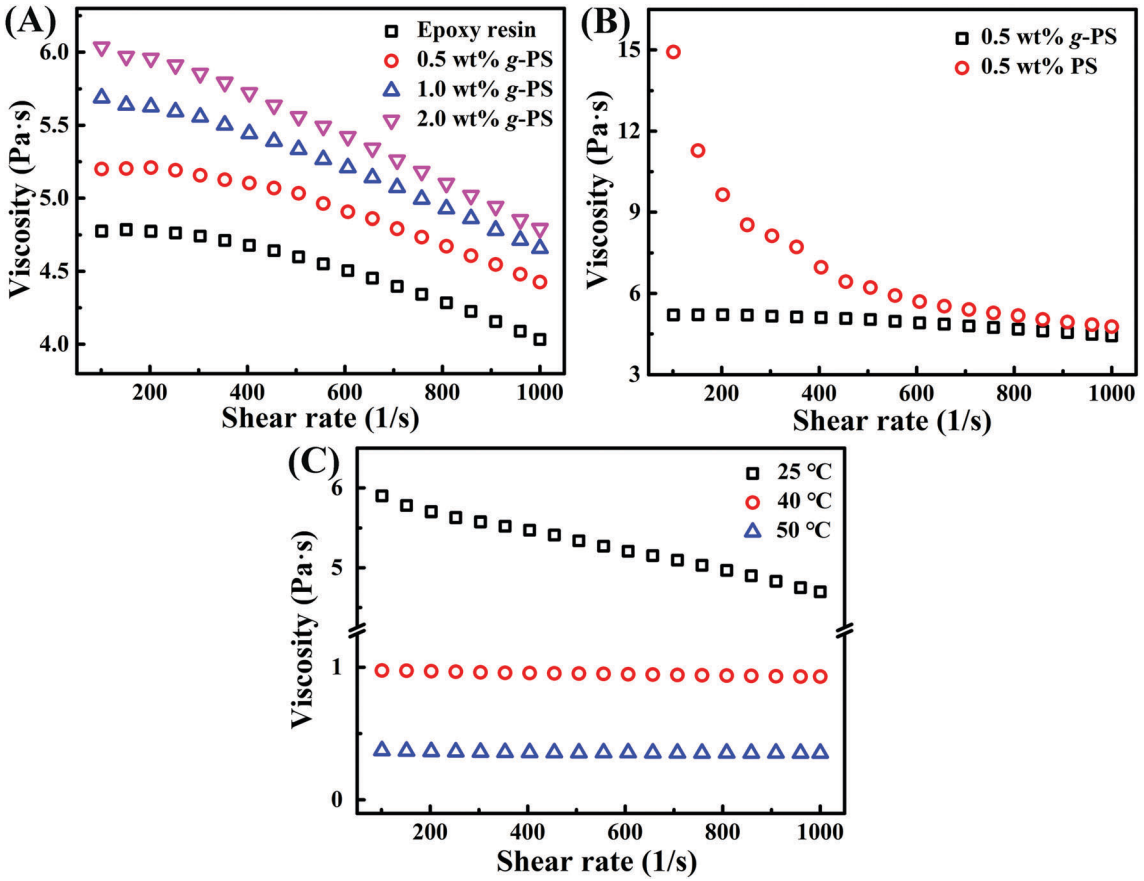

Fig. 3 (A) Viscosity *vs.* shear rate of epoxy resin suspensions with different loadings of *g*-PS at 25 °C; (B) effect of chemical grafting on the viscosity of epoxy resin suspension with 0.5 wt% loading of *g*-PS and PS at 25 °C; and (C) viscosity *vs.* shear rate of epoxy resin suspensions with 1.5 wt% loading of *g*-PS at temperatures of 25, 40, and 50 °C.

3.3 Viscosity of PS/epoxy composites

Fig. 3(A) shows the viscosity *vs.* shear rate for pure epoxy resin and its suspensions filled with different loadings of *g*-PS at 25 °C. It is observed that the viscosity of all of the suspensions exhibits the typical shear rate dependent property. For the pure epoxy resin, the shear rate dependent property is not that obvious as the shear rate is lower than 300 s^{-1}, and as the shear rate increases further, the viscosity is decreased obviously due to the entanglement of epoxy resin molecular chains with the shear rate.[28] For the epoxy suspensions with *g*-PS powders, the viscosity is sharply decreased with an increasing shear rate, exhibiting characteristic shear thinning behavior.[29] With the increase of the shear rate, the viscosity difference between epoxy suspensions and the different loadings of *g*-PS powders is diminished. Meanwhile, the viscosity is increased with increasing *g*-PS powder loadings. Presumably, this is due to the increased flow resistance of the laminar motion for the polymer chain after mixing *g*-PS with epoxy resin,[30] causing a higher viscosity relative to the pure epoxy resin. In Fig. 3(B), the viscosity for the epoxy resin suspensions with the 0.5 wt% loading of pure PS and *g*-PS powders is displayed. It is found that the viscosity of epoxy resin suspensions with pure PS is much higher than that of epoxy resin suspensions with *g*-PS, especially in the low shear rate range. After increasing the shear rate, this difference is decreased due to the shear thinning effect. It has been reported that the nanofillers with epoxide groups could help the nanofillers to disperse homogenously in the epoxy matrix because of the similar polarities of epoxide functionalized nanofillers and the epoxy matrix.[31] The decreased viscosity for the epoxy resin suspensions with *g*-PS compared with pure PS/epoxy resin suspensions may be a result of the improved compatibility between *g*-PS and epoxy resin and uniform dispersion of *g*-PS within the epoxy matrix, which could decrease the flow resistance of the epoxy monomer molecular chain with *g*-PS. This can also explain why the higher loading of pure PS/epoxy composites is hard to prepare since the viscosity is too high as mentioned in the experimental part.

Owing to the importance of temperature for the processability of epoxy,[32] the temperature effect on the viscosity of epoxy resin suspensions with *g*-PS is also investigated. The viscosity of epoxy resin suspensions with 1.5 wt% loading of *g*-PS at different temperatures is expressed in Fig. 3(C). The viscosity of epoxy resin suspensions with 1.5 wt% loading of *g*-PS powders conducted at 25, 40 and 50 °C is observed to be temperature dependent and decreases with increasing temperature. At 25 °C, the shear thinning phenomenon is still obvious for the epoxy resin suspensions. However, as the

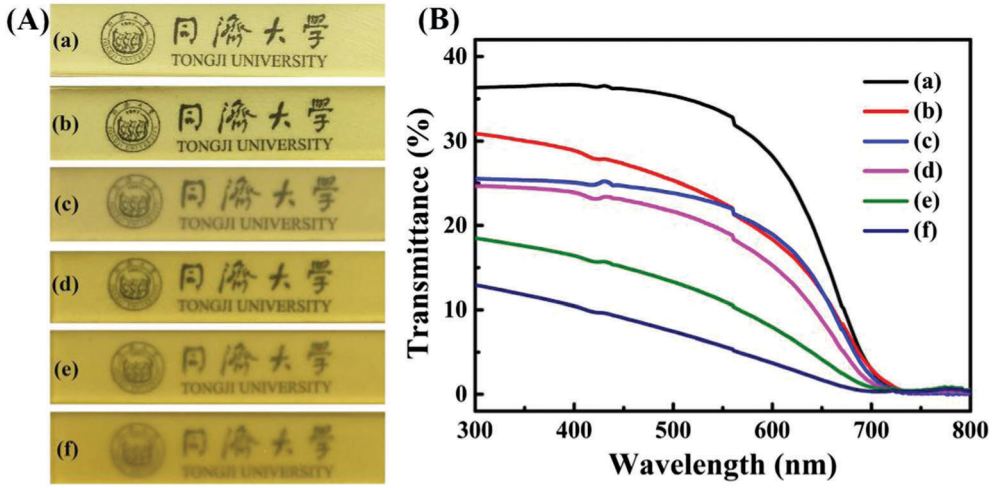

Fig. 4 (A) Digital photos and (B) transmittance curves for the cured (a) pure epoxy and epoxy composites filled with (b) 0.5 wt% *g*-PS, (c) 0.5 wt% PS (d) 1.0 wt% *g*-PS, (e) 1.5 wt% *g*-PS, (f) 2.0 wt% *g*-PS.

temperature increases to 40 and 50 °C, the viscosity for the epoxy resin suspensions is independent of the shear rate, which is almost close to the Newtonian behavior.

3.4 Transparency properties of PS/epoxy composites

The optically functional epoxy composites can be applied in optical materials such as displays, packaging materials and coatings.[33,34] In this work, the obtained epoxy composites with a low loading of PS exhibit high transparency properties in visible light. Fig. 4(A) shows the digital photos of cured pure epoxy and PS/epoxy composites, which are located on the paper with the printed words and logos ''Tongji University''. The corresponding transmittance curves of cured pure epoxy and PS/epoxy composites are depicted in Fig. 4(B). In Fig. 4(A), the background words ''Tongji University'' are clearly observed. This is an essentially important characteristic for the application of optical devices. In addition, it is found that the transparency of *g*-PS/epoxy composites is decreased with increasing *g*-PS loadings as shown in Fig. 4(A) and (B) (The transmittance for the cured pure epoxy and epoxy filled with *g*-PS loadings of 0.5, 1.0, 1.5, and 2.0 is 36.4, 30.9, 24.6, 18.5, and 12.9% at a wavelength of 300 nm, respectively.). Normally, transparent materials with multiple components are associated with the matching of refractive indices of different phases in these multiple components.[20] For the 0.5 wt% loading of *g*-PS/epoxy composites, Fig. 4(A) and (B)-b, the presence of epoxide groups makes *g*-PS possess similar polar and matching refractive indices to epoxy resin, leading to good transparency properties. Upon further increasing *g*-PS loadings, more *g*-PS phases are dispersed in the epoxy matrix, and more mismatching refractive indices are obtained, resulting in decreased transparency, Fig. 4(A) and (B)-d–f. The transmittance of the epoxy composites filled with 0.5 wt% loading of PS (Fig. 4(A) and (B)-c, 25.5%) is lower than that of epoxy composites filled with the same loading of *g*-PS (Fig. 4(A) and (B)-b, 30.9%), which is almost close to that of the epoxy composites filled with 1.0 wt% loading of *g*-PS (24.6%), Fig. 4(A) and (B)-d. The declined transparency of the pure PS/epoxy composites relative to the same loading of *g*-PS/epoxy composites is attributed to the poor compatibility and mismatching of refractive indices between pure PS and epoxy composites. It is also found that during the experiment for preparing *g*-PS/epoxy composites, after adding the curing agent, the epoxy suspensions became clearer under mechanical stirring. However, for the pure PS/epoxy suspension, the solution showed no obvious change during the mechanical stirring process. This can also confirm the improved compatibility between the *g*-PS and the epoxy matrix.

3.5 Tensile mechanical properties of PS/epoxy composites

The tensile strength and Young's modulus of cured pure epoxy and PS/epoxy composites were investigated by a unidirectional tensile test. The representative strain–stress curves of cured composites with different *g*-PS loadings are shown in Fig. 5(A) and the related tensile properties are summarized in Table 1. The tension variation curve with the error bars of cured epoxy composites filled with different loadings of *g*-PS is visually expressed in Fig. 5(B). The tensile strength (the maximum stress in the stress–strain curve, MPa) of the cured *g*-PS/epoxy composites shows the favorable effects of grafting on the reinforcement of cured epoxy. The tensile strength increases as *g*-PS loading increases to 1.5 wt%, and reduces as the loading reaches 2.5 wt%. The largest average tensile strength of cured epoxy composites is 97.4 MPa with a *g*-PS loading of 1.5 wt%, which is remarkably increased and 25.5% higher than that of cured pure epoxy (77.6 MPa). For the cured epoxy composites with a *g*-PS loading of 0.5, 1.0, 2.0 and 2.5 wt%, the tensile strength is observed to be 22.8 (95.3 MPa), 24.9 (96.9 MPa), 24.5 (96.6 MPa), and 9.5% (85.0 MPa) higher than that of cured pure epoxy, respectively. The Young's modulus (the slope of the stress–strain curve in the low strain range) of cured epoxy composites with *g*-PS shows no obvious differences from that of cured pure epoxy, while the Young's modulus of cured composites with 0.5 wt% loading of pure PS is 6.6% (2.25 GPa) lower than that of cured pure epoxy (2.41 GPa). The elongation-at-break

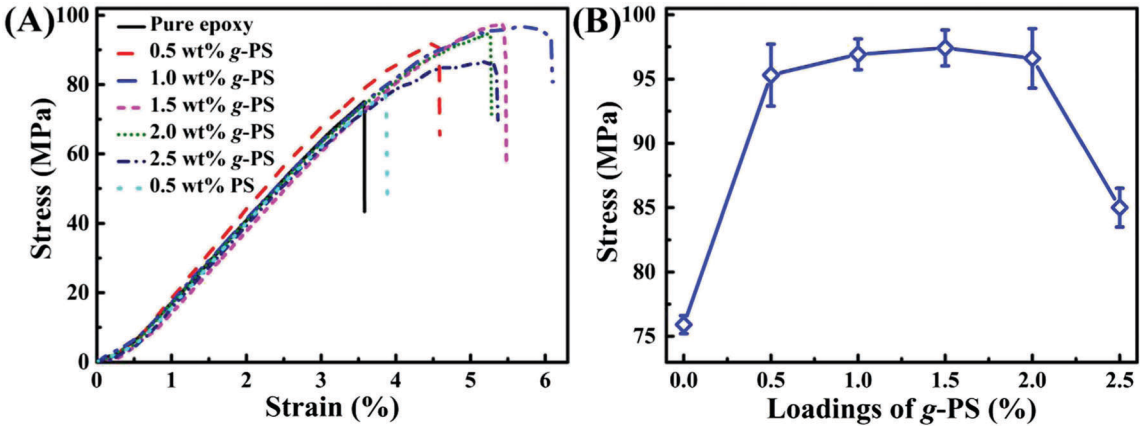

Fig. 5 (A) Stress–strain curves of cured epoxy composites filled with different loadings of *g*-PS and pure PS; (B) tensile strength with error bars of cured epoxy composites filled with different loadings of *g*-PS.

Table 1 Tensile mechanical properties of cured pure epoxy and epoxy composites

Sample	Tensile strength (MPa)	Young's modulus (GPa)	Elongation at break (%)
Pure epoxy	77.6 ± 0.7	2.43 ± 0.1	3.6 ± 0.1
Epoxy/0.5 wt% *g*-PS	95.3 ± 2.4	2.42 ± 0.2	6.0 ± 1.4
Epoxy/1.0 wt% *g*-PS	96.9 ± 1.2	2.43 ± 0.1	6.5 ± 0.4
Epoxy/1.5 wt% *g*-PS	97.4 ± 1.4	2.41 ± 0.1	5.6 ± 0.4
Epoxy/2.0 wt% *g*-PS	96.6 ± 2.3	2.36 ± 0.1	5.7 ± 0.4
Epoxy/2.5 wt% *g*-PS	85.0 ± 1.5	2.37 ± 0.1	5.3 ± 0.1
Epoxy/0.5 wt% PS	79.1 ± 4.1	2.25 ± 0.1	3.8 ± 0.4

of all of the cured epoxy and PS/epoxy composites is also listed in Table 1. It is observed that the elongation-at-break of all of the *g*-PS/epoxy composites is much higher than that of cured pure epoxy and PS/epoxy composites. The elongation-at-break for *g*-PS/epoxy composites is increased with *g*-PS loading up to 1.0 wt% and then declined upon further increasing the *g*-PS loadings, exhibiting an obvious toughening effect after grafting functional groups onto the PS polymer backbone. Normally, the modulus of toughness (U_t), which is used for describing the ability of materials to absorb energy and deform plastically without fracturing, is correlated with the area under the stress–strain curve.[35] The calculated U_t for the epoxy composites reinforced with *g*-PS loadings of 0.5, 1.0, 1.5, 2.0, and 2.5 wt% is 224.2, 355.9, 285.0, 273.7, and 268.7 MJ m^{-3} (or MPa), which is correspondingly 74.2, 176.6, 121.5, 112.7, and 108.9% larger than that of cured pure epoxy (128.7 MJ m^{-3}). The U_t for the 0.5 wt% loading of PS/epoxy composites is 147.6 MJ m^{-3}, which is much lower than that of *g*-PS/epoxy composites. The increased compatibility and chemical interaction between the *g*-PS and the epoxy matrix confirmed by contact angle and DSC tests are responsible for the increase of tensile strength and the modulus of toughness.

3.6 Microstructures of the fracture surface for PS/epoxy composites

Fig. 6 shows the SEM microstructures of the fracture surface for the cured epoxy and PS/epoxy composites. On the microscale, the cured pure epoxy exhibits a smooth fracture surface with "radiation-like" patterns, showing a typical brittle failure.[36] This is attributed to rapid crack propagation, Fig. 6(A and B). For the cured epoxy composites filled with 0.5 wt% of pure PS, Fig. 6(C and D), a rough surface is obtained and lots of PS holes are observed in the epoxy matrix. As an external tensile force was applied to the epoxy composites, the fracture energy could not be efficiently dissipated as a result of the weak interaction between pure PS powders and epoxy matrix. Therefore, the PS holes became the breaking points and the cracks were initiated from these holes as shown in an enlarged SEM image Fig. 6(D), leading to poor tensile strength as indicated in the tensile test, Fig. 5(A) and Table 1. However, the cured epoxy composites filled with 0.5 and 2.5 wt% of *g*-PS exhibit a totally different fracture surfaces from the pure epoxy and pure PS/epoxy composites, Fig. 6(E)–(H). It is observed that the holes from PS become fewer than those from the cured epoxy composites filled with 0.5 wt% of pure PS and numerous stereo dimples are present in the fracture surface of *g*-PS/epoxy composites due to the increased interfacial compatibility between the *g*-PS powders and the epoxy matrix, expressing a typical ductile failure.[37] The appearance of dimples means the formation of a new fracture surface, which can dissipate more energy and lead to increased tensile properties. A mechanism called "crack pinning" has been reported to explain the toughening mechanism of thermoplastic material modified epoxy.[38] According to this mechanism, the rigid *g*-PS powders could serve as impenetrable objects that caused the crack to bow out, which consumed extra energy. The observation of "tails" around PS holes as indicated by blue circles in Fig. 6(F) could confirm this mechanism. When the *g*-PS loading comes to 2.5 wt% of *g*-PS, Fig. 6(G) and (H), many white broken traces have been observed on the fracture surface of epoxy composites, which is probably from the agglomerated *g*-PS, making relatively lower tensile strength compared to those of the cured epoxy composites filled with low loadings of *g*-PS, Fig. 5(A) and Table 1.

3.7 Dynamic mechanical analysis of PS/epoxy composites

The temperature dependent storage modulus (G'), loss modulus (G''), and loss factor ($\tan\delta$) for the cured pure epoxy and epoxy

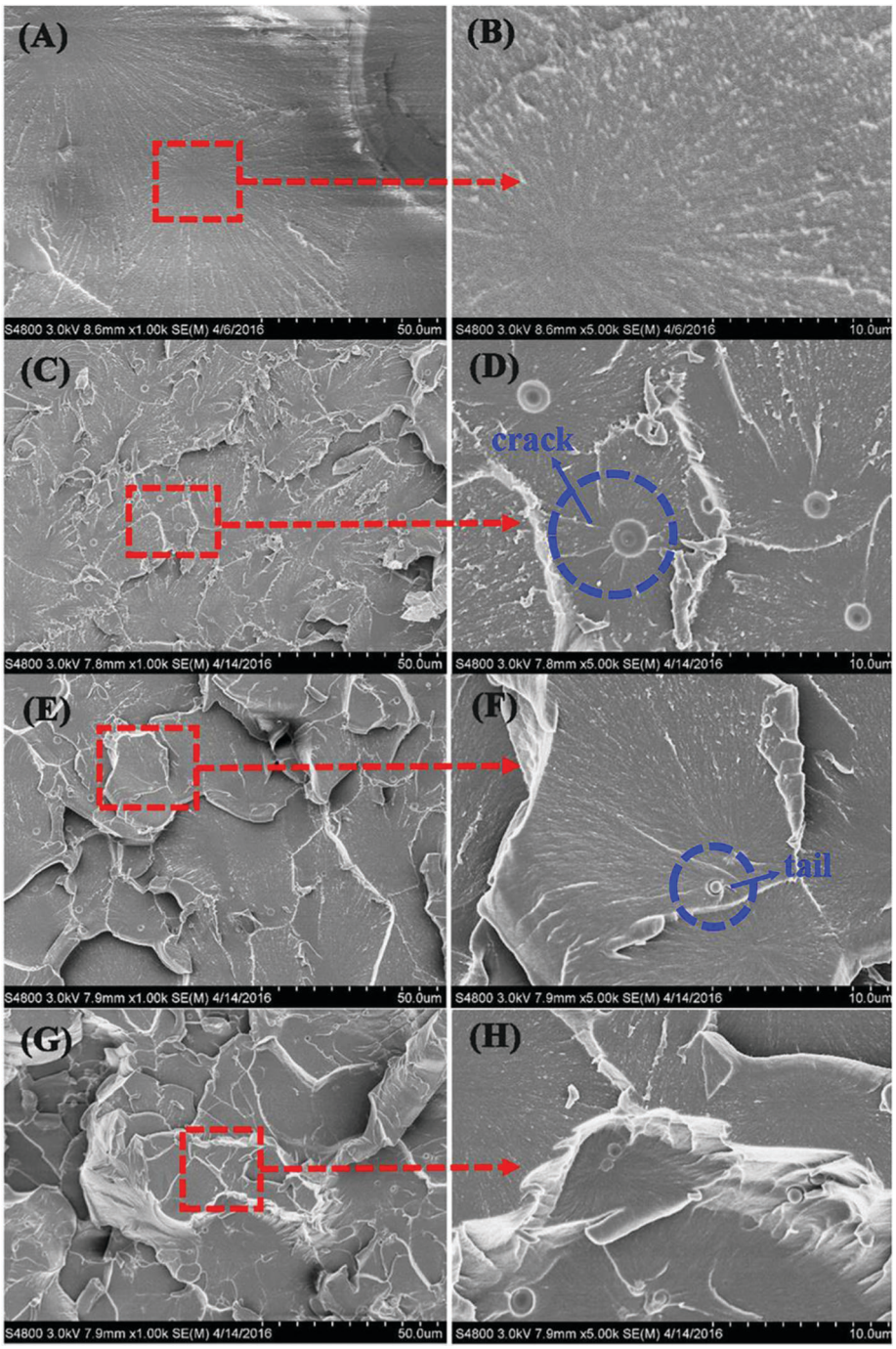

Fig. 6 SEM images of fracture surfaces for cured (A)&(B) pure epoxy, epoxy composites filled with (C)&(D) 0.5 wt% pure PS, (E)&(F) 0.5 and (G)&(H) 2.5 wt% *g*-PS.

composites filled with different loadings of *g*-PS powders are studied and the obtained results are displayed in Fig. 7. In Fig. 7(A), it is found that owing to energy dissipation, the G' for the cured pure epoxy and *g*-PS/epoxy composites is decreased with increasing temperature.[39] For the cured pure epoxy, the energy dissipation begins from 88.8 °C. However, this energy dissipation moves to a higher temperature of 12.1–17.4 °C for the epoxy filled with *g*-PS (103.0, 106.2, and 100.9 °C for epoxy composites filled with *g*-PS loadings of 0.5, 1.5, and 2.0 wt%, respectively) and the maximum value of G' is observed in the composites filled with 1.5 wt% loading of *g*-PS, which is consistent with the tensile tests. In Fig. 7(B), for the cured pure epoxy, the maximum peak of G'' is 99.7 °C. In comparison, for the *g*-PS/epoxy composites, this peak shifts to a higher temperature of 12.7–17.8 °C (113.8, 117.4, and 112.4 °C for epoxy composites filled with *g*-PS loadings of 0.5, 1.5 and 2.0 wt%, respectively). The glass transition temperature (T_g) of cured pure epoxy and *g*-PS/epoxy composites is the peak of the tan δ curve, Fig. 7(C).

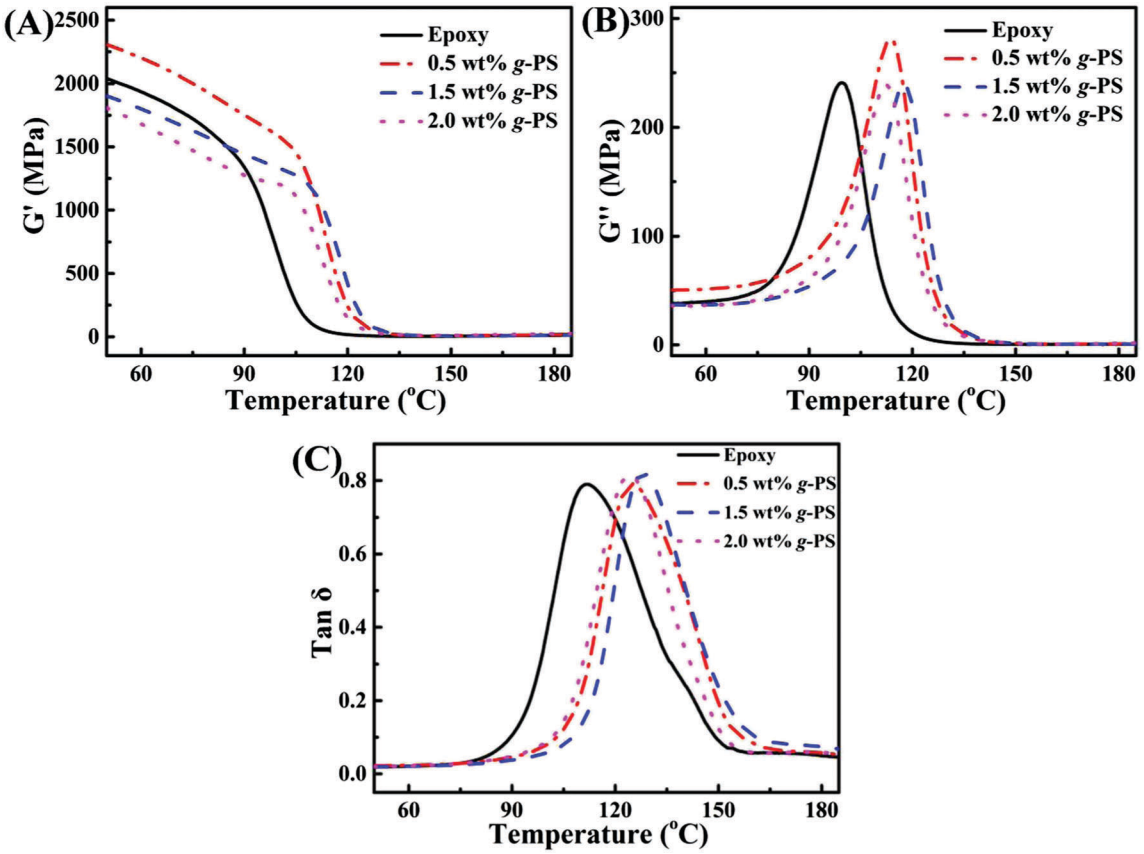

Fig. 7 (a) G', (b) G'' and (c) tan δ *vs.* temperature for the cured pure epoxy and epoxy composites with different loadings of *g*-PS.

The T_g of cured epoxy composites reinforced with *g*-PS loading of 0.5, 1.5 and 2.0 wt% is 125.1, 127.9, and 124.2 °C, respectively, which is 13.4, 16.2, and 12.5 °C higher than that of cured pure epoxy (111.7 °C). The increased T_g means good compatibility

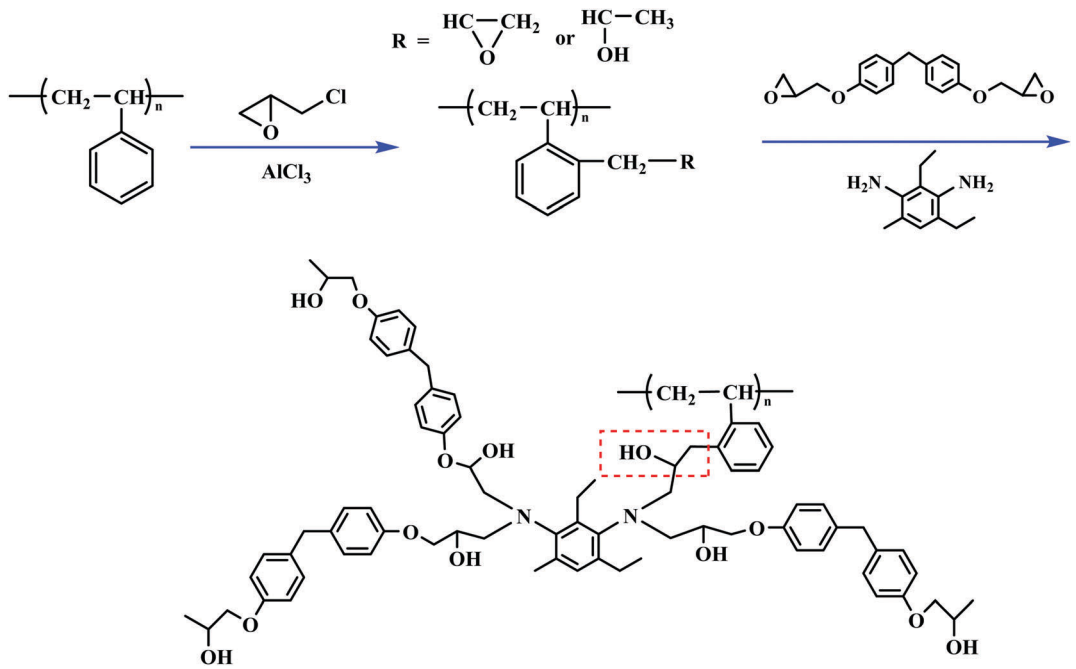

Scheme 1 Proposed curing mechanism for epoxy composites with *g*-PS.

between *g*-PS and the epoxy matrix, which could achieve a higher crosslinking density of epoxy and restrict the segmental movement of the polymer chain with increasing temperature.[40]

In summary, all of these results as aforementioned confirm that the grafting process helps the formation of the chemical interaction between *g*-PS and the epoxy matrix and attains the uniform dispersion of *g*-PS within the epoxy matrix due to the existence of hydroxyl and epoxide groups on the *g*-PS polymer backbone. The proposed crosslinking mechanism for this reinforcement effect is shown in Scheme 1.

4. Conclusion

Epichlorohydrin grafted PS (*g*-PS)/epoxy composites have been prepared at different powder loadings. The functional groups on the *g*-PS polymer backbone are hydroxyl and epoxide groups which have been confirmed by FTIR, TGA, and XPS analyses. The decreased surface tension and the exothermic peak in the DSC test indicate that *g*-PS could significantly improve the compatibility between *g*-PS and epoxy resin and chemically reacted with epoxy. The viscosity of *g*-PS/epoxy suspensions increases with increasing *g*-PS loadings and decreases with increasing shear rates. After grafting with functional groups, the viscosity for the *g*-PS/epoxy resin suspension is much lower than that of pure PS/epoxy suspensions due to a good dispersion quality of *g*-PS within the epoxy matrix. The *g*-PS/epoxy composites also exhibit good transparency compared with pure PS/epoxy composites. An enhancement of the mechanical properties by 25.5% has been achieved in the cured *g*-PS/epoxy composites compared with the cured pure epoxy. The significantly increased modulus of toughness for the cured *g*-PS/epoxy composites is much higher (increased by 176.6%) than that of cured pure epoxy (128.7 MJ m^{-3}). The rough fracture surface and less holes in the epoxy composites filled with *g*-PS indicate the efficient load transfer and uniform *g*-PS distribution. The DMA results show that after grafting with functional groups, the T_g of *g*-PS/epoxy composites moved to a higher temperature of 16.2 °C compared with that of cured pure epoxy (111.7 °C).

Acknowledgements

This work is supported by the Shanghai Science and Technology Commission (14DZ2261100). Dr Junwei Gu thanks the support and funding provided by the Foundation of National Natural Science Foundation of China (No. 51403175 and 81400765). Dr Hongbo Gu thanks the financial support from the Science and Technology Commission of Shanghai Municipality (No. 15YF1412700).

References

1 H. Gu, C. Ma, J. Gu, J. Guo, X. Yan, J. Huang, Q. Zhang and Z. Guo, *J. Mater. Chem. C*, 2016, **4**, 5890–5906.
2 N. Even, L. Adler-Abramovich, L. Buzhansky, H. Dodiuk and E. Gazit, *Small*, 2011, **7**, 1007–1011.
3 H. Jin, C. L. Mangun, D. S. Stradley, J. S. Moore, N. R. Sottos and S. R. White, *Polymer*, 2012, **53**, 581–587.
4 V. A. Agubra and H. V. Mahesh, *J. Polym. Sci., Part B: Polym. Phys.*, 2014, **52**, 1024–1029.
5 W. Tian, L. Liu, F. Meng, Y. Liu, Y. Li and F. Wang, *Corros. Sci.*, 2014, **86**, 81–92.
6 C. Bao, Y. Guo, L. Song, Y. Kan, X. Qian and Y. Hu, *J. Mater. Chem.*, 2011, **21**, 13290–13298.
7 T.-I. Yang, C.-W. Peng, Y. L. Lin, C.-J. Weng, G. Edgington, A. Mylonakis, T.-C. Huang, C.-H. Hsu, J.-M. Yeh and Y. Wei, *J. Mater. Chem.*, 2012, **22**, 15845–15852.
8 P. Jyotishkumar, J. Koetz, B. Tiersch, V. Strehmel, C. Özdilek, P. Moldenaers, R. Hässler and S. Thomas, *J. Phys. Chem. B*, 2009, **113**, 5418–5430.
9 J. Gu, X. Yang, C. Li and K. Kou, *Ind. Eng. Chem. Res.*, 2016, **55**, 10941–10946.
10 G. Li, Z. Huang, C. Xin, P. Li, X. Jia, B. Wang, Y. He, S. Ryu and X. Yang, *Mater. Chem. Phys.*, 2009, **118**, 398–404.
11 L. Sobrinho, V. Calado and F. Bastian, *Polym. Compos.*, 2012, **33**, 295–305.
12 B. Francis, V. L. Rao, S. Jose, B. K. Catherine, R. Ramaswamy, J. Jose and S. Thomas, *J. Mater. Sci.*, 2006, **41**, 5467–5479.
13 S. K. Shukla and D. Srivastava, *J. Mater. Sci.*, 2007, **42**, 3215–3222.
14 L. H. Sinh, B. T. Son, N. N. Trung, D.-G. Lim, S. Shin and J.-Y. Bae, *React. Funct. Polym.*, 2012, **72**, 542–548.
15 P. K. Roy, N. Iqbal, D. Kumar and C. Rajagopal, *J. Cleaner Prod.*, 2014, **21**, 1–9.
16 A. Zabaniotou and E. Kassidi, *J. Cleaner Prod.*, 2003, **11**, 549–559.
17 M. Tawfik and A. Huyghebaert, *Food Addit. Contam.*, 1998, **15**, 592–599.
18 A. Cundell, *Mar. Pollut. Bull.*, 1973, **4**, 187–188.
19 B. G. Kwon, K. Saido, K. Koizumi, H. Sato, N. Ogawa, S.-Y. Chung, T. Kusui, Y. Kodera and K. Kogure, *Environ. Pollut.*, 2014, **188**, 45–49.
20 C. Hoppe, M. Galante, P. Oyanguren, R. Williams, E. Girard-Reydet and J. Pascault, *Polym. Eng. Sci.*, 2002, **42**, 2361–2368.
21 T. Sun, Z. Wu, Q. Zhuo, X. Liu, Z. Wang and H. Fan, *Composites, Part A*, 2014, **66**, 58–64.
22 A. C. Baudouin, J. Devaux and C. Bailly, *Polymer*, 2010, **51**, 1341–1354.
23 H. Gu, S. B. Rapole, Y. Huang, D. Cao, Z. Luo, S. Wei and Z. Guo, *J. Mater. Chem. A*, 2013, **1**, 2011–2021.
24 H. Gu, H. Lou, J. Tian, S. Liu and Y. Tang, *J. Mater. Chem. A*, 2016, **4**, 10174–10185.
25 J. Schultz and M. Nardin, *Handbook of adhesive technology*, 1994, pp. 19–33.
26 K. L. Mittal and A. Pizzi, *Adhesion promotion techniques: technological applications*, Marcel Dekker, 1999.
27 J. Jang, J. Bae and K. Lee, *Polymer*, 2005, **46**, 3677–3684.
28 H. Gu, S. Tadakamalla, X. Zhang, Y.-D. Huang, Y. Jiang, H. A. Colorado, Z. Luo, S. Wei and Z. Guo, *J. Mater. Chem. C*, 2013, **1**, 729–743.
29 P. Pötschke, T. D. Fornes and D. R. Paul, *Polymer*, 2002, **43**, 3247–3255.
30 J. Zhu, S. Wei, J. Ryu, L. Sun, Z. Luo and Z. Guo, *ACS Appl. Mater. Interfaces*, 2010, **2**, 2100–2107.

31 L. Chen, C. Zhang, Z. Du, H. Li and W. Zou, *Mater. Lett.*, 2013, **110**, 208–211.
32 M. H. Pahl and D. Hesekamp, *Rheology*, 1993, **3**, 97–104.
33 J. Zhu, S. Wei, M. J. Alexander, T. D. Dang, T. C. Ho and Z. Guo, *Adv. Funct. Mater.*, 2010, **20**, 3076–3084.
34 Y. Li, H. Zhu, H. Gu, H. Dai, Z. Fang, N. J. Weadock, Z. Guo and L. Hu, *J. Mater. Chem. A*, 2013, **1**, 15278–15283.
35 H. Gu, J. Guo, H. Wei, S. Guo, J. Liu, Y. Huang, M. A. Khan, X. Wang, D. P. Young and S. Wei, *Adv. Mater.*, 2015, **27**, 6277–6282.
36 J. Gu, C. Liang, X. Zhao, B. Gan, H. Qiu, Y. Guo, X. Yang, Q. Zhang and D.-Y. Wang, *Compos. Sci. Technol.*, 2017, **139**, 83–89.
37 J. Gu, X. Meng, Y. Tang, Y. Li, Q. Zhuang and J. Kong, *Composites, Part A*, 2017, **92**, 27–32.
38 R. A. Pearson and A. F. Yee, *Polymer*, 1993, **34**, 3658–3670.
39 Q.-P. Feng, X.-J. Shen, J.-P. Yang, S.-Y. Fu, Y.-W. Mai and K. Friedrich, *Polymer*, 2011, **52**, 6037–6045.
40 H.-B. Hsueh and C.-Y. Chen, *Polymer*, 2003, **44**, 5275–5283.